

SOFT-SWITCHING BIDIRECTIONAL DC/DC CONVERTER AS A TRANSFORMER

Babitha Pattayil

Dept.Of Electrical and ElectronicsEngineering
 MEA Engineering College,Perinthalmanna

Muhammedali Shafeeque

Assistant Professor
 MEA Engineering College,Perinthalmanna

Abstract— In this paper a soft-switching bidirectional dc/dc converter acts as a dc –dc transformer is proposed which can do all the functions of buck and boost converter. In this paper soft switching is done by using LC series resonant circuit. Soft switching is done at ZVS conditions. The proposed topology do functions by minimizing all the problems of hard switching.. A zero voltage switching operation of the power switches reduces the switching loss during the switching transition and improves the overall efficiency Simulation is done in PSIM.

Keywords— Battery charger, bidirectional dc/dc converter, resonant converter, soft switching.

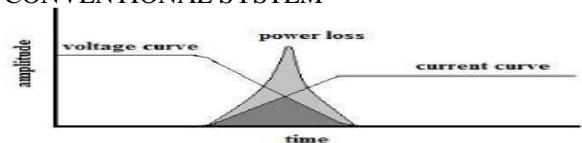
1. INTRODUCTION

The bidirectional dc-dc converter has been widely studied for various industrial applications such as renewable energy system, hybrid electric vehicles and uninterruptible power supplies system [1]–[7]. The conventional type DC/DC converter incorporating the old switching techniques would raise the switching losses and voltage stresses on the devices. The above drawback is rectified with the help of soft switching techniques. The buck-boost converter topology allow power flow in either direction, i.e., toward battery or away from battery. To reduce the corresponding switching losses and the size of passive components, soft switching techniques are required. In some conventional bidirectional buck-boost converter topologies applied with hard-switching technique not only the resonant components but also additional power switching devices are required. For energy effective charging and discharging system, some of bidirectional converter topologies have been studied [8], [9]. Among the various topologies, transformer-based structures are prob- ably the most popular topologies. However, these topologies with isolated transformers have high-conduction losses, because the usual number of power switches is between four and nine [10]–[14].All these drawbacks are also avoided by using this topology.

2. RELATED WORKS

A detailed comparison between hard switching and soft switching is done. Its action as a transformer ie,in buck and boost mode operation is work out.

3. CONVENTIONAL SYSTEM

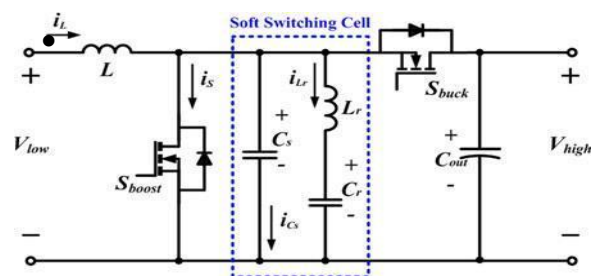


Fig(1)Hard switching phenomenon

In the traditional PWM converters operating on hard switching, where the current and voltage pulses goes from high to low value or from low to high value during the transition period, switching loss occurs. Also generate a substantial amount of Electromagnetic interference. These losses arise because of output capacitor of transistor, capacitance of diode and diode reverse recovery. From observation, it is seen that the switching loss is directly proportional to the switching frequency. So the higher switching loss limits the switching frequency to a minimum value. Because of wide spectral range of harmonics present in PWM waveform, a high Electro Magnetic Interference (EMI) occurs. Current spikes caused by Diode recovery can also result in this EMI. Soft switching techniques can reduce the switching losses and Electromagnetic interference by putting some stress on the devices.

4. PROPOSED SYSTEM

I .SOFT-SWITCHING BIDIRECTIONAL DC/DC CONVERTER



Fig(3)proposed converter system

The number of circuit elements is simple to configure. So mode of operation is simple. Also, the loss caused by the devices small. Above all, the biggest advantage, proposed topology is possible to achieve high efficiency at light load. Types of soft switching techniques are: Zero voltage switching (ZVS) . Zero current switching (ZCS).

Here we use only ZVS. In this technique, the switching takes place at zero voltage condition. It is used at turning OFF of the device. Initially the device is conducting. So the current through the device is not zero but the voltage across it is zero.

5. OPERATION PRINCIPLE

A. Proposed Converter Configuration

Figure(2) shows a schematic of the proposed bidirectional dc/dc converter of new soft-switching cell. The soft switching of the proposed converter is achieved by LC resonance. The proposed converter is based on the conventional bidirectional buck–boost converter. The soft-switching cell that consists of a snubber capacitor C_s , a resonant inductor L_r , and a resonant capacitor C_r is added. In the boost mode, the snubber capacitor C_s induces the switch Sboost to turn OFF under ZVS condition by changing the current path flowing to switch. The ZVS condition is achieved by series resonance between resonant inductor and resonant capacitor.

B. Soft-Switching Principles

Actually, the ZVS condition can be achieved when the current of resonant inductor is larger than that of main inductor. The current of resonant inductor can be increased by series resonance between resonant inductor and capacitor during the switch-off time interval. The snubber capacitor can be fully discharged by the difference between currents of resonant inductor and of main inductor. After the discharge of snubber capacitor, the excessive current flow conducts the anti parallel diode of the main switch. Consequently, the ZVS condition of main switch can be satisfied due to the excessive current flow. The turn-off signal of main switch has to be supplied during this time interval for ZVS.

C. Operation Mode

To simplify the analysis of the proposed converter, some the circuit operates under steady state; all of the switches are considered as ideal devices; the parasitic capacitances of switches are equal; all of energy storage components are free of loss. The operation mode of proposed topology is divided into seven modes. Fig. 4 shows the operation mode and key waveforms of the proposed converter in buck mode during a single switching period. Fig.5 shows the operation mode and key waveforms of the proposed converter in buck mode during a single switching period.

Mode 1 ($t_0 \leq t < t_1$): Mode 1 starts when the switch Sboost is turned ON. The main inductor current i_L flows to switch Sboost and resonant circuit. During this mode, the resonant inductor current i_{Lr} decreases to zero. When the resonant capacitor C_r is fully charged, mode 1 is finished.

$$i_{Lr}(t) = i_L(t_0) \cos \omega_r t - \frac{v_{C_r}(t_0)}{Z_r} \sin \omega_r t \quad (1)$$

$$v_{C_r}(t) = v_{C_r}(t_0) \cdot \cos \omega_r t + i_L(t_0) \cdot Z_r \sin \omega_r t. \quad (2)$$

Mode 2 ($t_1 \leq t < t_2$): At time t_1 , the direction of i_{Lr} is

current flows to the switch Sboost.

$$i_{Lr}(t) = -\frac{v_{C_r}(t_1)}{Z_r} \sin \omega_r t \quad (4)$$

$$v_{C_r}(t) = v_{C_r}(t_1) \cdot \cos \omega_r t. \quad (5)$$

Mode 3 ($t_2 \leq t < t_3$): This mode is started when the switch Sboost is turned OFF with ZVS condition and current flows to snubber capacitor C_s . Switch Sboost is zero voltage state. The voltage of snubber capacitor increases to output voltage V_{out}

$$i_{Lr}(t) = \frac{C}{C_s} i_L(t_2) + \left(i_{Lr}(t_2) - \frac{C}{C_s} i_L(t_2) \right) \cos \omega_a t - \frac{v_{C_r}(t_2)}{Z_a} \sin \omega_a t \quad (6)$$

$$v_{C_r}(t) = \frac{i_L(t_2)}{C_r + C_s} t + \frac{C}{C_s} \cdot v_{C_r}(t_2) \cdot \left(1 + \frac{C_s}{C_r} \cos \omega_a t \right) + \frac{C}{C_r} Z_a \left(i_{Lr}(t_2) - \frac{C}{C_s} i_L(t_2) \right) \sin \omega_a t \quad (7)$$

$$v_{C_s}(t) = \frac{i_L(t_2)}{C_r + C_s} t + \frac{C}{C_s} \cdot v_{C_r}(t_2) \cdot (1 - \cos \omega_a t) + \frac{C}{C_s} Z_a \left(\frac{C}{C_s} i_L(t_2) - i_{Lr}(t_2) \right) \sin \omega_a t \quad (8)$$

Mode 4 ($t_3 \leq t < t_4$): At time t_3 , the voltage across C_s is equal to V_{out} and antiparallel diode of Sboost is turned ON. The charged energy of the main inductor L and the resonant circuit is transmitted to the load through antiparallel diode of Sboost.

$$i_{Lr}(t) = i_{Lr}(t_3) \cdot \cos \omega_r t + \frac{V_o - v_{C_r}(t_3)}{Z_r} \sin \omega_r t \quad (9)$$

$$v_{C_r}(t) = V_o - (V_o - v_{C_r}(t_3)) \cos \omega_r t + i_{Lr}(t_3) \cdot Z_r \sin \omega_r t. \quad (10)$$

Mode 5 ($t_4 \leq t < t_5$): The main inductor current i_L flows to the resonant circuit and the load. The main inductor current i_L is decreased and resonant inductor current i_{Lr} is increased.

$$i_{Lr}(t) = \frac{V_o - v_{C_r}(t_4)}{Z_r} \sin \omega_r t \quad (11)$$

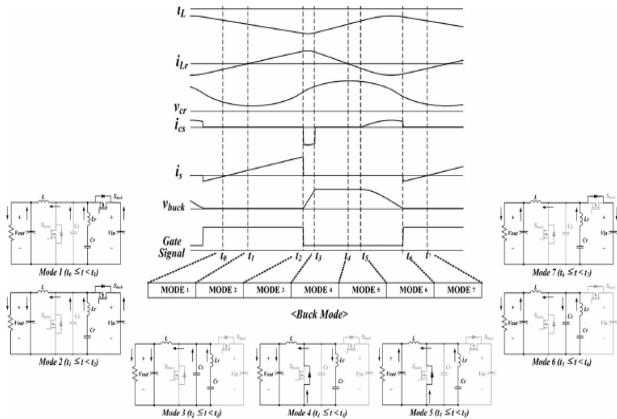
$$v_{C_r}(t) = V_o - (V_o - v_{C_r}(t_4)) \cdot \cos \omega_r t. \quad (12)$$

Mode 6 ($t_5 \leq t < t_6$): Mode 6 starts with discharge of C_s . When the voltage across C_s becomes lower than V_{out} antiparallel diode of Sboost turns OFF. And mode 6 ends,

$$i_{L_r}(t) = \frac{C}{C_s} i_L(t_5) \left(1 + \frac{C_s}{C_r} \cos \omega_a t \right) + \frac{V_o - v_{C_r}(t_5)}{Z_a} \sin \omega_a t \quad (13)$$

$$v_{C_r}(t) = \frac{I_L(t_5)}{C_r + C_s} t + v_{C_r}(t_5) + \frac{C}{C_r} (V_o - v_{C_r}(t_5)) (1 - \cos \omega_a t) + \left(\frac{C}{C_r} \right)^2 i_L(t_5) Z_a \sin \omega_a t \quad (14)$$

$$v_{C_s}(t) = \frac{i_L(t_5)}{C_r + C_s} t + \frac{C}{C_r} V_o \left(1 + \frac{C_r}{C_s} \cos \omega_a t \right) + \frac{C}{C_s} \cdot v_{C_r}(t_5) \cdot (1 - \cos \omega_a t) - \frac{C}{C_r + C_s} i_L(t_5) Z_a \sin \omega_a t. \quad (15)$$

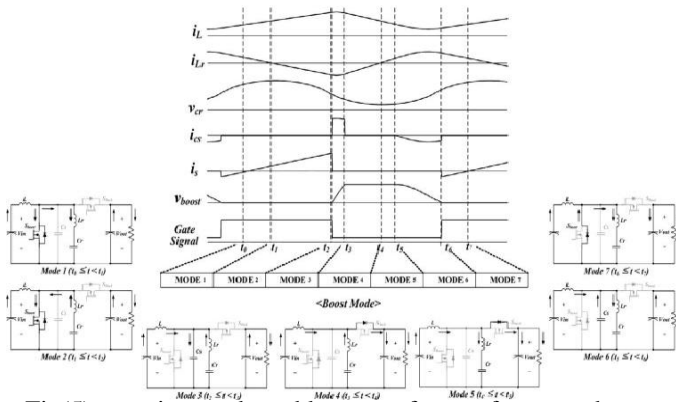


Fig(4)operation mode and key waveforms of proposed converter in buck mode

Mode 7 ($t_6 \leq t < t_7$): When i_{L_r} flows to antiparallel diode of switch S_{boost} and voltage of C_s is fully discharged, this mode starts. The switch S_{buck} is turned ON with ZVS condition. When antiparallel diode of switch S_{boost} turns OFF, mode 7 ends.

$$i_{L_r}(t) = i_{L_r}(t_6) \cos \omega_r t - \frac{v_{C_r}(t_6)}{Z_r} \sin \omega_r t \quad (16)$$

$$v_{C_r}(t) = v_{C_r}(t_6) \cdot \cos \omega_r t + i_{L_r}(t_6) \cdot Z_r \sin \omega_r t. \quad (17)$$



Fig(5)operation mode and key waveforms of proposed converter in boost mode

6. CONTROL OF THE PROPOSED DC/DC CONVERTER

For ZVS operation of the proposed converter, the switch-off time has to be determined according to the LC series resonant period. When the voltage of switch is zero, the switch is turned

ON and maintains on state during set time.

7. DESIGN OF RESONANT ELEMENTS

Since the proposed converter turned ON and OFF under ZVS condition by using resonance without an auxiliary switch, the design of resonant components is important to ensure the ZVS condition.

Fig. 7 shows the voltage and current waveforms related to the resonance. When the switch is ON, the current toward the switch flows into the snubber capacitor, so the process of the switch ON is made in the state that the switch is zero voltage. When the resonant inductor current is greater than the main inductor current during the switch-off time, the current difference comes to form the current path through the snubber capacitor. During this time interval, the snubber capacitor is fully discharged to zero voltage.

A. Design of Resonant Inductor

The current variation of resonant inductor current to satisfy the resonant condition has to be greater than main inductor current ripple as represented in (18). The minimum value of main inductor current can be represented as (19), and the maximum value of resonant inductor current can be represented as (20). By substituting the (19) and (20) into the (18), the maximum value of resonant inductance can be derived as (21)

$$I_{L_min} \leq I_{L_r_peak} \quad (18)$$

$$I_{L_min} = \frac{V_{out}}{V_{in}} \times I_O - \frac{T_{on}}{2 \cdot L} \cdot V_{in} \quad (19)$$

$$I_{L_r_peak} = \frac{1}{2} \cdot \frac{V_{in}}{L_r} \cdot T_{on} \quad (20)$$

$$L_r \leq \frac{V_{in} \cdot L \cdot T_{on}}{2 \cdot G_v \cdot L - V_{in} \cdot T_{on}} \quad (21)$$

B. Design of Resonant Capacitor

To achieve the ZVS operation, the resonant frequency should be lower than a half of switching frequency. In this paper, the resonant frequency is selected as 40% of the switching frequency. It can be represented as (22). After the design of resonant inductance, the resonant capacitance can be determined according to the selected resonant frequency as shown in (23).

$$\frac{2.5}{2 \cdot \sqrt{L_r \cdot C_r}} \leq f_{sw} \quad (22)$$

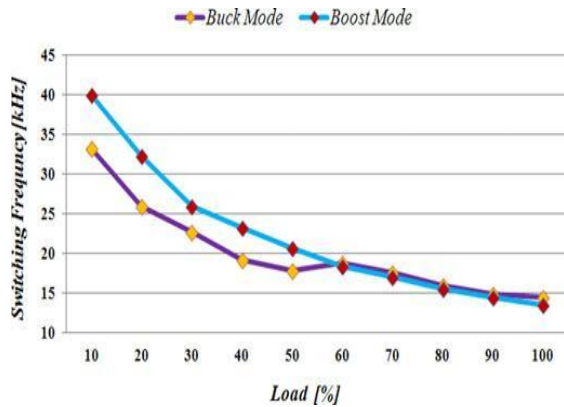
$$C_r \leq \frac{0.25}{4 \cdot \pi^2 \cdot L_r \cdot f_{sw}^2} \quad (23)$$

C. Design of Snubber Capacitor

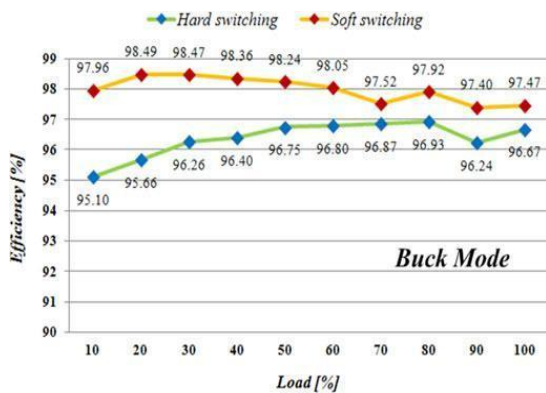
The snubber capacitor voltage is recharged to the output voltage during turn-off interval, and it is discharged to zero voltage by the difference between resonant inductor current and the main inductor at the section of t_4 – t_5 of boost action Mode 5. Since the larger snubber capacitance causes the increase of resonant current to ensure ZVS condition, not only

the main inductor current but also the resonant current has to be considered for snubber capacitor design. In this paper, the snubber capacitance is selected so that the time for the switch to be the state of zero potential is within 3 μs. The design equation for snubber capacitor can be represented as (24).

$$C_s \leq \frac{1}{V_{out}} \cdot \int_{t_s}^{t_e} (I_{Lr} - I_L) dt. \quad (24)$$



Fig(6) Switching frequency with load variation



Fig(8) Efficiency variation with Load in buck mode

figure (8) shows the efficiency characteristics in both soft switching and hard switching. Which shows that soft switching is most efficient.

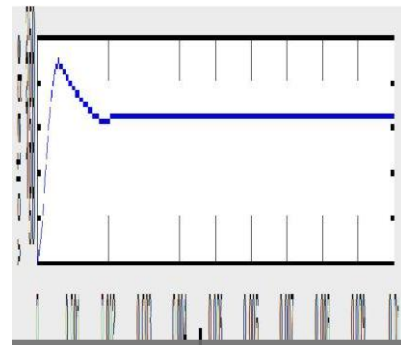
8. SIMULATION RESULTS

A computer simulation for operational characteristics of other proposed dc/dc converter is executed by using Physical Security Information Management (PSIM) software. The simulation parameters are shown in Table I.

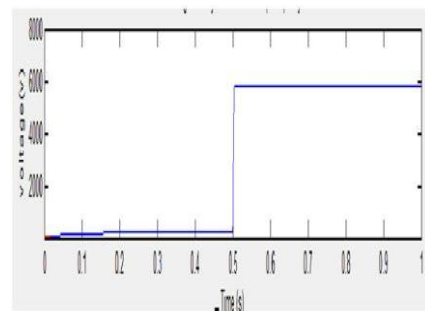
TABLE I
 BOOST MODE OF SIMULATION PARAMETERS

Parameter	Value	Unit
Main inductor L	700	μH
Resonant inductor L_r	489	μH
Snubber capacitor C_s	33	nF
Resonant capacitor C_r	2	μF
Output capacitor C_{out}	900	μF
Input / Output voltage	200 / 400	V
Rated output power	2	kW

The proposed converter gives the input voltage 200 [V]. The output voltage is controlled to dc 400 [V] of constant voltage. The simulation circuit and corresponding waveform is shown below. The proposed converter action in buck and boost mode with soft switching is shown below.



Fig(9) softswitching in buck mode.



Fig(10) soft switching in boost mode

9. CONCLUSION AND SCOPE OF SEMINAR.

In this paper, a soft-switching bidirectional buck boost converter fed PMDC motor with an LC series resonant circuit for the battery charge and discharge system of dc distribution power system is proposed. The proposed topology is analyzed using the circuit analysis method of operating mode. The designed proposed topology is simulated using PSIM simulation software program. The various waveforms obtained for changes in load. The simulation results show ZVS turn ON. Based on the analysis, the proposed converter has been obtained for soft switching at all over load of bidirectional. The switches are turned ON and OFF under zero-voltage condition by adding the LC series resonant circuit to the conventional bidirectional the design of LC resonant component is also considered. The proposed topology is verified through simulation result and it can be applied to the renewable energy system using battery with high efficiency.

REFERENCES

[1] H.-J. Chiu and L.-W. Lin, "A bidirectional DC-DC converter for fuel cell electric vehicle driving system," IEEE Trans. Power Electron., vol. 21, no. 4, pp. 950-958, Jul. 2006.

[2] S. D. G. Jayasinghe, D. M. Vilathgamuwa, and U. K. Madawala, "Diode-clamped three-level inverter-based battery/supercapacitor direct integration scheme for renewable energy systems," IEEE Trans. Power Electron., vol. 26, no. 12, pp. 3720-3729, Dec. 2011.

[3]J. Cao and A. Emadi, "A new battery/ultra capacitor hybrid energy storage system for electric, hybrid, and plug-in hybrid electric vehicles," *IEEE Trans. Ind. Electron.*, vol. 27, no. 1, pp. 122–132, Jan. 2012.

[4]S. J. Chiang, K. T. Chang, and C. Y. Yen, "Residential photovoltaic energy storage system," *IEEE Trans. Ind. Electron.*, vol. 45, no. 3, pp. 385–394, Jun. 1998.

[5]F. Z. Peng, M. Shen, and K. Holland, "Application of Z-source inverter for traction drive of fuel cell–battery hybrid electric vehicles," *IEEE Trans. Ind. Electron.*, vol. 22, no. 3, pp. 1054–1061, May 2007.

[6]M. Arias, M. M. Hernando, D. G. Lamar, J. Sebastián, and A. Fernández, "Elimination of the transfer-time effects in line-interactive and passive standby UPSs by means of a small-size inverter," *IEEE Trans. Ind. Electron.*, vol. 27, no. 3, pp. 850–862, Apr. 2010.

[7]L. Schuch, C. Rech, H. L. Hey, H. A. Grundling, H. Pinheiro, and J. R. Pinheiro, "Analysis and design of a new high-efficiency bidirectional integrated ZVT PWM converter for DC-bus and battery-bank interface," *IEEE Trans. Ind. Electron.*, vol. 42, no. 5, pp. 1321–1332, Sep./Oct. 2006.

[8]D. V. Ghodke, K. Chatterjee, and B. G. Fernandes, "Modified One-cycle controlled bidirectional high-power-factor AC-to-DC converter," *IEEE Trans. Ind. Electron.*, vol. 55, no. 6, pp. 2459–2472, Jun. 2008.

[9]R.-J. Wai and R.-Y. Duan, "High-efficiency bidirectional converter for power sources with great voltage diversity," *IEEE Trans. Power Electron.*, vol. 22, no. 5, pp. 1986–1996, Sep. 2007.

[10] H. S.-H. Chung, W.-L. Cheung, and K. S. Tang, "A ZCS bidirectional flyback DC/DC converter," *IEEE Trans. Power Electron.*, vol. 19, no. 6, pp. 1426–1434, Nov. 2004.

[11]C. Yao, X. Ruan, X. Wang, and C. K. "Isolated buckboos DC/DC converters suitable for wide input-voltage range," *IEEE Trans. Power Electron.*, vol. 26, no. 9, pp. 2599–2613, Sep. 2011.

[12] Boonyaroonate and S. Mori, "Analysis and design of class E isolated DC/DC converter using class E low dv/dt PWM synchronous rectifier," *IEEE Trans. Power Electron.*, vol. 16, no. 4, pp. 514–521, Jul. 2001.

[13]J.-Y. Lee, Y.-S. Jeong, and B.-M. Han, "An isolated DC/DC converter using high-frequency unregulated resonant converter for fuel cell applications," *IEEE Trans. Ind. Electron.*, vol. 58, no. 7, pp. 2926–2934, Jul. 2011.

[14]D. Vinnikov and I. Roasto, "Quasi-Z-source-based isolated DC/DC converters for distributed power generation," *IEEE Trans. Ind. Electron.*, vol. 58, no. 1, pp. 192–201, Jan. 2011.

[15]P. Das, S. A. Mousavi, and G. Moschopoulos, "Analysis and design of a nonisolated bidirectional ZVS-PWM DC–DC converter with coupled inductors," *IEEE Trans. Power Electron.*, vol. 25, no. 10, pp. 2630–2641, Oct. 2010.

[16]H. Wu, J. Lu, W. Shi, and Y. Xing, "Nonisolated bidirectional DC–DC converters with negative-coupled inductor," *IEEE Trans. Power Electron.*, vol. 27, no. 5, pp. 2231–2235, May 2012.

[17]P. Das, B. Laan, S. A. Mousavi, and G. Moschopoulos, "A nonisolated bidirectional ZVS-PWM active clamped DC–DC converter," *IEEE Trans. Power Electron.*, vol. 24, no. 2, pp. 553–558, Feb. 2009.